

Mechanism of Cathodic Reactions in Acetic Acid Corrosion of Iron and Mild Steel

Aria Kahyarian,^{‡,*} Bruce Brown,^{*} and Srdjan Nešić^{*}

ABSTRACT

The mechanism of the cathodic reaction in acetic acid corrosion of iron and API X65 mild steel was investigated in mildly acidic sodium chloride electrolytes. The behavior of the charge transfer controlled currents in the steady state voltammograms showed that undissociated acetic acid is not significantly electroactive. This behavior was found to be in accordance with the so-called “buffering effect” mechanism, where acetic acid acts solely as an additional source of hydrogen ions. The increased limiting currents in the presence of acetic acid showed a linear correlation with undissociated acetic acid concentration in agreement with the Levich equation, suggesting that the limiting currents are under mass transfer control. Both pure iron and X65 steel exhibited a similar behavior regarding the cathodic currents, indicating that the mechanism of hydrogen ion reduction is not influenced by minor impurities present in the X65 steel.

KEY WORDS: acetic acid, acidic corrosion, aqueous environments, cathodic polarization, mechanism, mild steel, uniform corrosion

INTRODUCTION

The mechanisms of cathodic reactions in aqueous corroding systems and the presence of weak acids have been the subject of numerous studies.¹⁻⁸

Carbonic acid, hydrogen sulfide, and organic acids are the most common weak acids found in oil and gas production, transmission, and processing infrastructure. It is well known that corrosion rate in the presence of these weak acids is significantly higher when compared to strong acids at the same pH.⁹⁻¹⁰ Therefore, a mechanistic understanding of the role of these weak acids in increasing the corrosion rate is crucial for accurate corrosion rate estimation and, thus, for effective corrosion mitigation strategies.

Reports on the significance of organic acids in corrosion of pipeline steel can be found as early as the 1940's.¹¹ It was suggested that small concentrations of organic acids (300 mass ppm) can cause severe corrosion of pipeline steel.¹¹ At the same time, studies on the formation water composition found in oil and gas wells reported organic acid concentrations in the range of several hundred milligrams per liter.¹²⁻¹⁴ Because of its prevalence,¹⁵ the effect of acetic acid (HAc) on mild steel corrosion has frequently been studied as the representative organic acid.¹⁵⁻²⁰

The partial dissociation of weak acids has generally been considered to be the main factor responsible for the increased corrosion rates. Unlike strong acids, weak acids only partially dissociate in an aqueous solution. Hence, the dissolved weak acid is present in both its dissociated and undissociated forms. This chemical equilibrium for acetic acid is shown by Reaction (1):



Submitted for publication: June 20, 2016. Revised and accepted: July 25, 2016. Preprint available online: July 25, 2016, <http://dx.doi.org/10.5006/2177>.

[‡] Corresponding author. E-mail: ak702711@ohio.edu.

^{*} Institute for Corrosion and Multiphase Flow Technology, Department of Chemical and Biomolecular Engineering, Ohio University, Athens, OH.

Reaction (1) is mathematically described by Equation (2), where K_{HAc} is the corresponding equilibrium constant, i.e., 1.75×10^{-5} (M) at 25°C.⁵

$$K_{\text{HAc}} = \frac{[\text{H}^+][\text{Ac}^-]}{[\text{HAc}]} \quad (2)$$

The effect of acetic acid on the corrosion of mild steel has been extensively studied.^{2,15-17,21-26} Based on an analogy with other weak acids, such as carbonic acid and hydrogen sulfide, the increased corrosion rates in the presence of acetic acid were conventionally associated with the electroactivity of the undissociated acetic acid.^{22,25,27-31} Garsany, et al.,²¹ studied the reduction reactions of sodium chloride solutions containing acetic acid and carbon dioxide on platinum and API X65 mild steel electrodes. The reported limiting currents were found to correspond with the mass transfer of acetic acid. However, the authors suggest that the underlying charge transfer process cannot be distinguished from that of hydrogen ion reduction at such conditions because of the fast kinetics of acetic acid dissociation. The authors also reported a double wave in their voltammograms obtained on X65 mild steel in acetic acid containing solutions. It was suggested that both waves are a result of the reduction of acetic acid, while the rate limiting process is different. That is, the first wave is caused by charge transfer limitation, probably a result of a change in the reaction mechanism, and the second wave is the mass transfer limitation of the electroactive species.²¹ In 2007, George and Nešić²² studied the effect of acetic acid on the carbon dioxide corrosion of mild steel using a series of potentiodynamic sweeps and corrosion rate data. It was reported that the observed corrosion rates significantly increased in the presence of acetic acid, which was found to be more profound at higher temperatures (60°C). Therefore, authors concluded that the undissociated acetic acid was directly reduced at the metal surface.²² Using a similar approach, Okafor, et al.,²⁸ studied the effect of acetic acid on carbon dioxide corrosion in an extended temperature (up to 80°C) and acetic acid concentration (5,000 mass ppm) ranges. The authors concluded that undissociated acetic acid was directly reduced and further proposed a reaction mechanism that included a surface dissociation of adsorbed acetic acid followed by an electron transfer reaction.²⁸ A generally similar argument and experimental approach, leading to the same conclusion (direct acetic acid reduction), is frequent in the literature.^{15,17,25,30,32} This corrosion mechanism presumes two parallel cathodic reactions, namely, hydrogen ion reduction (Reaction [3]) and acetic acid direct reduction (Reaction [4]). This reaction pathway is referred to as the “direct reduction” mechanism.^{2,33}



The development of comprehensive mathematical models in the early 2000's provided the opportunity for detailed quantitative analysis of the water chemistry inside the diffusion layer.^{5,34-36} This included the ability to account for the effect of homogeneous reactions related to the presence of weak acids on the chemistry of the solution adjacent to the metal surface. These studies showed that the undissociated weak acid not only buffers the *bulk* solution, but can also act as a reservoir of hydrogen ions at the *metal surface* as they are consumed during the corrosion process.^{5,33,35,37}

In mildly acidic environments, the decay of the surface hydrogen ion concentration as a result of its consumption by the corrosion process plays a significant role in limiting the corrosion rate.³⁸⁻³⁹ In strong acid solutions, mass transfer from the bulk is the only means of supplying the hydrogen ions to the surface. However, the presence of undissociated weak acids provides an additional source of hydrogen ions through the dissociation reaction. This is a result of the shift in the equilibrium by decreased hydrogen ion concentration (Reaction [1]). Therefore, the hydrogen ion concentration at the metal surface is buffered, which in turn results in increased corrosion rates under such conditions.

Over the last decade, the ability of weak acids (such as acetic acid and carbonic acid) to buffer the surface pH was emphasized to the extent that suggests the direct reduction of the undissociated acid does not have a significant role in the increased corrosion rates. In 2011, Amri, et al., studied the effect of acetic acid on the top of the line corrosion of mild steel.²⁶ The authors reported that at conditions where the corrosion current was under charge transfer control, the presence of acetic acid had no significant influence on the corrosion rate, concluding that the undissociated acetic acid was not electrochemically active.²⁶ In 2013, Tran, et al.,² investigated the mechanism of steel corrosion in the presence of acetic acid in more detail. The authors suggested using stainless steel as a more noble electrode material in order to remove the interference by the iron dissolution reaction. This resulted in voltammograms with charge transfer cathodic currents over a wider potential range. The reported results in that study indicated a clear Tafel behavior of the cathodic currents, as the signature of pure charge transfer control. Furthermore, the charge transfer controlled currents showed no significant response to increasing concentrations of acetic acid up to 1,000 ppm (mass). Therefore, it was concluded that direct reduction of acetic acid was insignificant. The reasoning behind this argument is discussed later in detail. These recent studies suggest that the only cathodic reaction involved in the corrosion process is the hydrogen ion reduction, while the role of acetic acid is buffering the hydrogen ion concentration through the dissociation reaction.^{1-2,40} This reaction mechanism is referred to as the “buffering effect” mechanism.^{1-2,33,40}

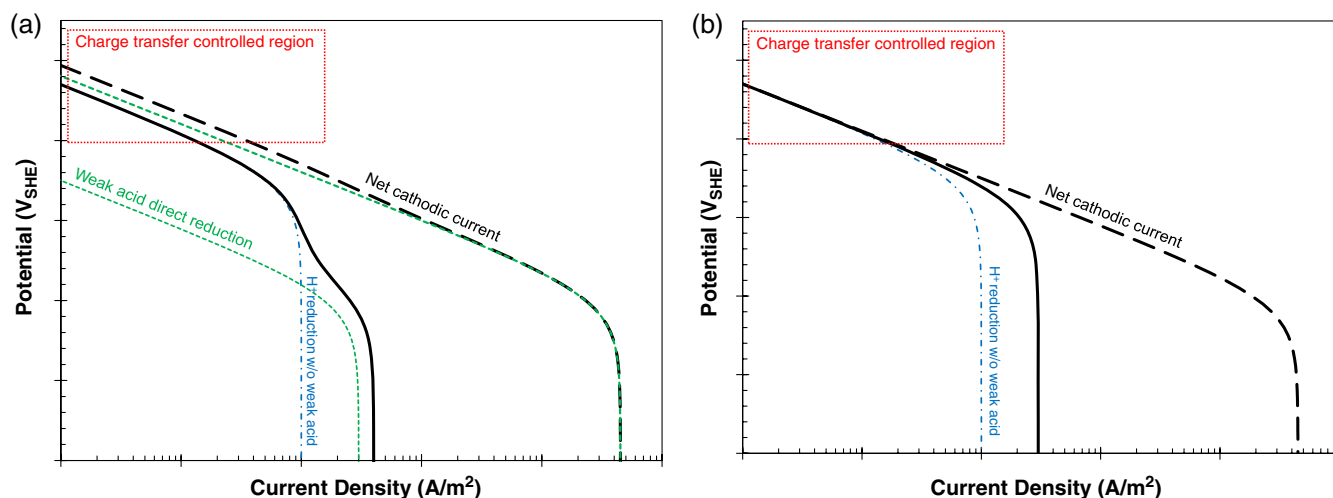


FIGURE 1. Illustration of the hypothetical cathodic polarization curves at a constant pH and two different concentrations of a weak acid (solid black line < dashed black line). Black lines: net current, dotted-dashed blue lines: H^+ reduction without weak acid present, and dashed green lines: weak acid direct reduction. (a) Direct reduction mechanism and (b) buffering effect mechanism.

In the discussion above, the buffering effect and direct reduction are not two mutually exclusive mechanisms; rather, they can be seen as two possible pathways for the hydrogen evolution reaction. Note that the direct reduction mechanism is related to the electroactivity of the undissociated weak acid, while the buffering effect mechanism is related to the dissociation of the weak acid inside the diffusion layer. Nevertheless, as discussed in this short review, the relative significance of these two reaction pathways for acetic acid has been disputed.^{1-2,26,40}

These two mechanisms (direct reduction and buffering effect) are compared in Figure 1, where their corresponding hypothetical polarization curves are illustrated for two extreme cases. The first case (Figure 1[a]) shows the condition where the weak acid is electrochemically active and is directly reduced, while it has no buffering ability. The second case is the condition where the weak acid is not electroactive and the only cathodic reaction is the hydrogen ion reduction, while the weak acid can readily dissociate to buffer the surface pH (Figure 1[b]). The governing mechanism of the cathodic reaction in the presence of a weak acid can be differentiated by the behavior of the cathodic voltammograms at various undissociated weak acid concentrations and at a constant pH, as shown in Figure 1. Depending on the chemical and electrochemical properties of a weak acid, different characteristic polarization behavior is expected, both in the mass transfer controlled and charge transfer controlled currents.

For the first case (Figure 1[a]), the weak acid reduction and hydrogen ion reduction are two independent electrochemical reactions. Therefore, a “double wave” in the mass transfer controlled currents of the polarization curves can be observed in a certain concentration range of the weak acid. This behavior

stems from two distinct limiting currents, one for hydrogen ion reduction and the other for weak acid direct reduction. Hydrogen sulfide is an example of one such weak acid, where a double wave similar to what is schematically shown in Figure 1(a) was observed.^{3,6-7,41} This double wave was shown to be associated with the mass transfer limiting currents of hydrogen ion reduction and hydrogen sulfide direct reduction.³

While the presence of the double wave is a strong indication of the weak acid direct reduction, its absence is not conclusive evidence for dismissing this reaction. The latter can be the case where the weak acid is also a strong buffer, i.e., it can readily dissociate. In such conditions, regardless of the electroactivity of the weak acid, the limiting current behavior is similar to that of the second case, as shown in Figure 1(b). Here, the electrochemical activity of a weak acid can be investigated based on the characteristic behavior of the charge transfer controlled currents for the two cases discussed above. This concept is also illustrated in Figure 1 by showing the distinct behavior of the charge transfer currents at different weak acid concentrations. In the case where the direct reduction of the weak acid is significant, the charge transfer controlled cathodic current (in the area denoted by the box in Figure 1) should increase at higher weak acid concentrations, as depicted in Figure 1(a). On the other hand, when the weak acid is not electrochemically active, and hydrogen ions are the only reducible species, the charge transfer controlled current should remain unaffected by the change in weak acid concentration, as shown in Figure 1(b).

The main obstacle in verification of these two hypothetical behaviors is related to the difficulty in observing the pure charge transfer controlled

cathodic currents in typical corrosion experiments.^{16,22,25,28} This is a result of the interference of the iron dissolution reaction, which obscures the cathodic currents in the potential range where they are under charge transfer control. As mentioned, this issue has been addressed in the studies of Tran, et al.,^{2,40} by using stainless steel electrodes. However, considering the effect of the alloying compounds (~20 wt% Cr and 10 wt% Ni²⁺) and the passive layer on the electroactivity of the metal surface, possibly changing the mechanism of the cathodic reactions, the experimental findings on stainless steel should not be considered valid for mild steel without further verification.

Using an improved experimental apparatus, the present research investigated this hypotheses using pure iron and X65 steel electrodes in order to directly verify the mechanism proposed by Tran, et al.,² without the complicating effect introduced by using a stainless steel electrode.

MATERIALS AND METHODS

All experiments were conducted using a conventional 2 L, three-electrode glass cell. A saturated Ag/AgCl reference electrode was connected to the cell through a Luggin capillary. The counter electrode was a platinum wire with significantly higher surface area than the working electrode. The working electrodes were made from 99.99% pure iron or X65 steel (see Table 1 for the chemical composition). These electrodes were 5 mm in diameter, press fit into PTFE rotating disk electrode (RDE) holders. Each electrode was initially abraded using 1000 grit silicon carbide paper and then mirror polished using successively finer silicon suspensions down to 0.25 μm . Electrodes were then rinsed and sonicated in isopropanol and further electrochemically cleaned prior to each test with a series of decreasing magnitude galvanic steps ($\pm 5 \text{ A/m}^2$, $\pm 2 \text{ A/m}^2$, and $\pm 1 \text{ A/m}^2$) in the study solution. Each step was 60 s long, followed by 120 s rest at zero current. Finally, the electrode was left at open-circuit potential (OCP) for 20 min before potential sweep measurement was taken. This electrochemical cleaning procedure was devised based on the thermodynamic stability of the iron oxide layer,⁴² and implemented in order to enhance the removal of any iron oxide layer that may have formed during electrode preparation. Considering the reported iron/iron oxide Pourbaix diagrams in aqueous environments,⁴² iron (III) oxide is thermodynamically unstable in the pH and the potential range of the present study. Therefore, the oxide layer is spontaneously reduced to ferrous ions, which can be further kinetically

TABLE 1

Chemical Composition of the X65 Mild Steel in wt%

S	P	V	C	Cr	Mo	Si	Ni	Mn	Fe
0.009	0.009	0.047	0.13	0.14	0.16	0.26	0.36	1.16	Balance

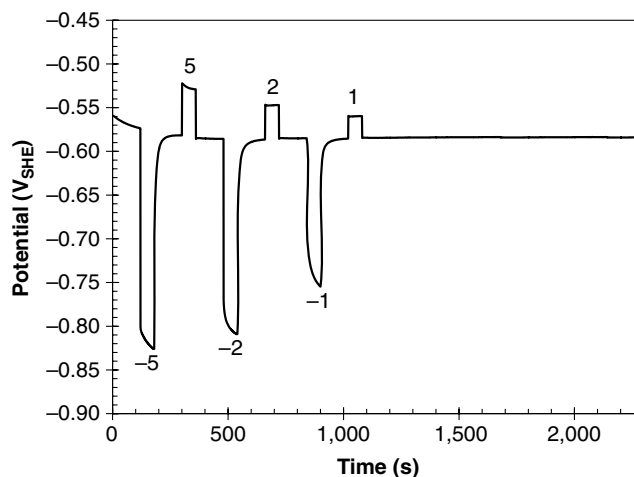


FIGURE 2. Electrode potential during the electrochemical cleaning procedure on an iron electrode at pH 5, 25°C, 2,000 rpm RDE, and 1 wt% NaCl. Labels are the applied current densities in A/m^2 .

enhanced by polarizing the electrode cathodically. On the other hand, the anodic polarizations were considered to minimize the adsorption/absorption of the hydrogen atoms that are produced during the cathodic polarization, knowing that the formation of any solid products during this step is thermodynamically infeasible at the conditions of the present study. Figure 2 demonstrates the polarization behavior of an iron electrode during this cleaning process.

The potential sweep measurements were conducted at 1 mV/s scan rate. The voltammograms reported in the present study were corrected for ohmic drop using the solution resistance obtained at high-frequency range electrochemical impedance measurements obtained after each potential sweep measurement.

The supporting electrolyte was 1 wt% NaCl in deionized water, and was used throughout this study. The acetic acid concentrations reported in the present work are the amount of the acid added into the solution, which correspond to the total concentration of acetate species. After adding the desired amount of acetic acid, the pH was adjusted using dilute NaOH or HCl solutions as required. Finally, the electrolyte was deaerated by purging the solution with nitrogen gas for at least 120 min prior to inserting the working electrode.

As noted, the acetic acid concentration reported in the present study is the sum of its dissociated and undissociated forms, or in other words, the total concentration of acetate species (C_t). The concentration of undissociated acid at a known pH can be calculated based on Equation (2) and mass conservation, as follows:

$$[\text{HAc}] = \frac{C_t [\text{H}^+]}{K_{\text{HAc}} + [\text{H}^+]} \quad (5)$$

Equation (5) suggests that at pH 4, 85% of the total acetic acid in the solution is in undissociated form,

TABLE 2
Summary of the Experimental Conditions

Experimental Conditions	
Test apparatus	Rotating disk electrode Three-electrode glass cell
Temperature	25°C
Rotation rate	2,000 rpm
Electrode material	Pure iron, X65 mild steel
Supporting electrolyte	1 wt% NaCl
pH	4.0, 5.0
Total acetate concentration	0 mass ppm 100 mass ppm (1.66 mM) 500 mass ppm (8.30 mM) 1,000 mass ppm (16.60 mM)

while at pH 5, this value decreased to 36%. A summary of the experimental conditions can be found in Table 2.

RESULTS AND DISCUSSION

The voltammograms reported in Figures 3 and 5 show that using RDE working electrodes with high rotation speed enabled observation of Tafel behavior for the cathodic reaction by increasing the mass transfer limiting current. The steady state voltammograms obtained at pH 4 and pH 5 on iron electrodes are shown in Figure 3. The charge transfer controlled cathodic currents observed in Figure 3 show no significant variation at different acetic acid concentrations. This behavior was in accordance with the buffering effect mechanism, as shown in Figure 1(b), which is a similar behavior as reported by Tran, et al., on stainless steel electrodes.² The only apparent discrepancy between the hypothesized and observed behavior was seen at pH 5 in the absence of acetic acid, where significantly lower cathodic currents were observed. This was a result of mass transfer controlled current over the entire cathodic range of potentials in this particular

condition. On the other hand, the anodic branches of the voltammograms shown in Figure 3 were shifted toward lower current densities as the concentration of acetic acid was increased. This same behavior has been reported in the literature, suggesting that acetic acid slightly retards the iron dissolution reaction.^{15,25-26}

The OCPs reported in Figure 3 were also slightly shifted toward more positive potentials with increasing acetic acid concentrations. This was found to be in accordance with the above discussion, where the charge transfer controlled cathodic currents in the vicinity of OCP were not affected by increased acetic acid concentrations, while the anodic currents were slightly inhibited at higher acetic acid concentrations. Therefore, their intersect (OCP) was expected to slightly shift toward more positive potentials with increased acetic acid concentrations, a similar behavior as observed in Figure 3.

The comparison of limiting currents in Figures 3(a) and (b), where no acetic acid was present, showed an order of magnitude increase with decreasing pH from 5 to 4. That was the behavior expected from Levich equation describing the mass transfer limiting current density (i_{lim} A/m²) for an RDE⁴³ with conversion to SI units:

$$i_{lim} = 0.62 \times 10^3 n F D^{2/3} \omega^{1/2} \nu^{-1/6} C_b \quad (6)$$

where C_b (M) is the bulk concentration of the reactant and D (m²/s) is its diffusion coefficient, ν (m²/s) is the kinematic viscosity of the solution, ω (rad/s) is angular velocity, F (C/mol) is Faraday's constant, and n is the number of electron transferred.

Figure 4 shows the increase of the limiting current in the presence of acetic acid versus the concentration of the undissociated acetic acid in a log-log plot. Considering that the slope of the trendline in this graph is nearly unity (1.02), the increase of the

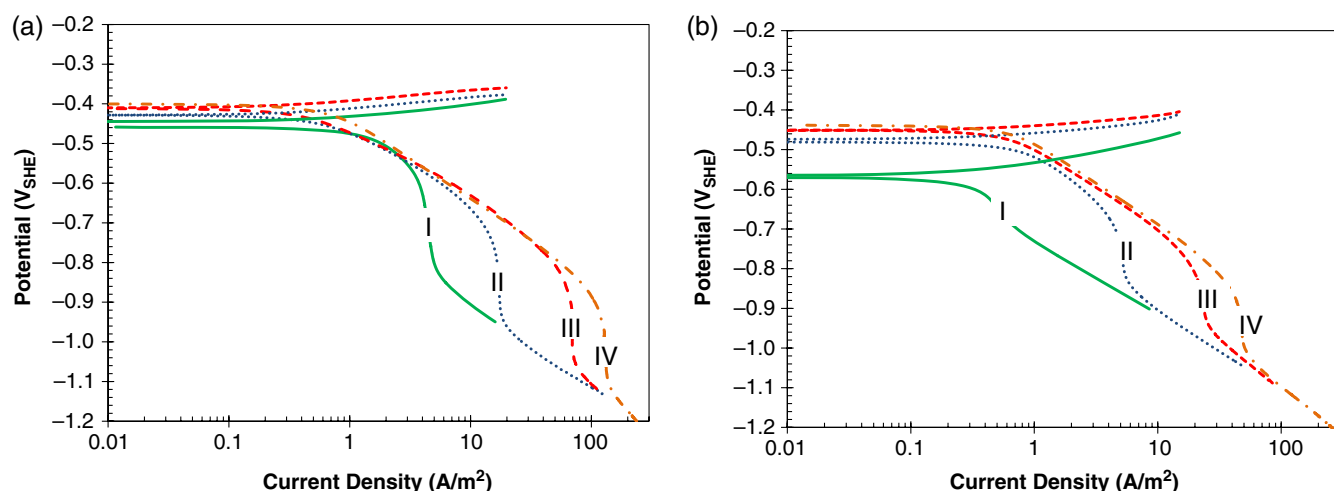


FIGURE 3. Polarization curves obtained on iron at 25°C, 2,000 rpm RDE, 1 wt% NaCl, and various total acetate concentrations. I: 0 mM, II: 1.66 mM, III: 8.30 mM, and IV: 16.60 mM. (a) pH 4 and (b) pH 5.

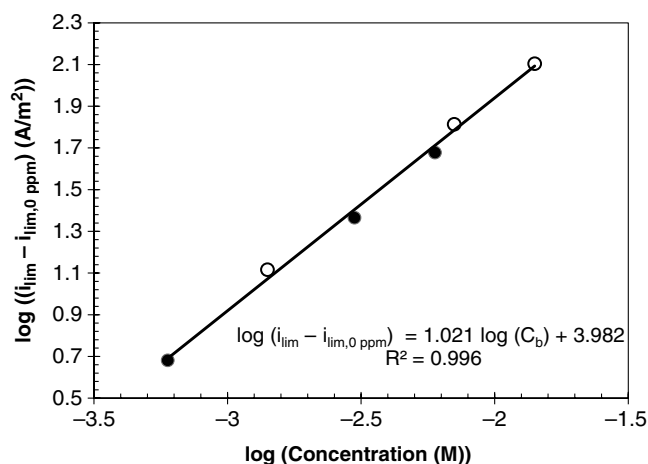


FIGURE 4. The increase in the limiting current density at various concentrations of undissociated acetic acid reported in Figure 3, obtained on iron at 25°C, 2,000 rpm RDE, and 1 wt% NaCl. Open circles: pH 4, closed circles: pH 5. The trendline is shown as the solid line with the equation at the bottom.

limiting current resulting from the presence of acetic acid was in linear correlation with the concentration of undissociated acetic acid ($R^2 = 0.996$), regardless of the bulk pH. Furthermore, the intercept of the trendline (3.98) was found to agree well with the theoretically obtained value of 4.01 from Levich equation (Equation [6]) (diffusion coefficient and water kinematic viscosity from Nordsveen, et al.⁵). This agreement indicated that the measured limiting currents are under pure mass transfer control; thus, the surface concentration of undissociated acetic acid was negligibly small. The latter further suggests that the kinetics of the preceding acetic acid dissociation reaction (Reaction [1]) is not rate determining.

Figure 5 shows the voltammograms obtained on X65 steel electrode. A similar behavior of the limiting current with respect to both pH and undissociated weak acid concentration was observed on X65 steel as that of iron electrodes. The pure charge transfer controlled currents for the cathodic reactions on X65 steel were also not significantly affected by acetic acid concentration, in accordance with the buffering effect mechanism. The slightly retarded anodic currents and the behavior of the OCP with increasing concentrations of acetic acid on X65 steel were also similar to that seen on iron electrodes.

The cathodic currents observed on pure iron and X65 steel in acid solution and the presence of acetic acid are directly compared in Figure 6. A similar limiting current was observed on both X65 steel and pure iron, as expected. Additionally, the charge transfer controlled currents showed similar behavior for both metals, suggesting that the mechanism of the hydrogen evolution reaction from hydrogen ions and water was the same on pure iron and X65 steel. However, the cathodic currents of the hydrogen ion reduction, as well as water reduction on X65 steel, are higher than that observed on iron. This suggests X65 mild steel is a more active catalyst for these reactions, which is in accordance with the behavior previously reported on the iron electrodes containing alloying impurities by Bockris and Drazic.⁴⁴

An example of the repeatability of the cathodic polarization measurements is shown in Figure 7 for both pure iron and X65 electrodes at pH 5 in the presence of acetic acid. The error bars represent the standard deviation of the current density at selected potentials for at least three measurements. Generally a similar variation range was observed throughout the measurements, while the reproducibility was slightly decreased in higher pH values and higher acetic acid concentrations.

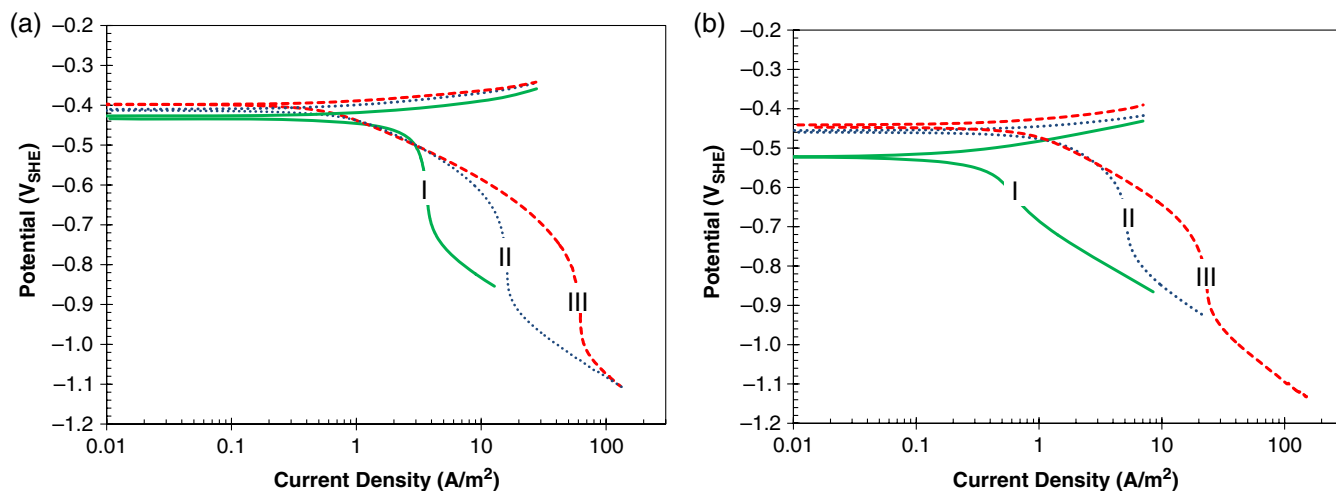


FIGURE 5. Polarization curves obtained on X65 mild steel at 25°C, 2,000 rpm RDE, 1 wt% NaCl, and various total acetate concentrations. I: 0 mM, II: 1.66 mM, and III: 8.30 mM. (a) pH 4 and (b) pH 5.

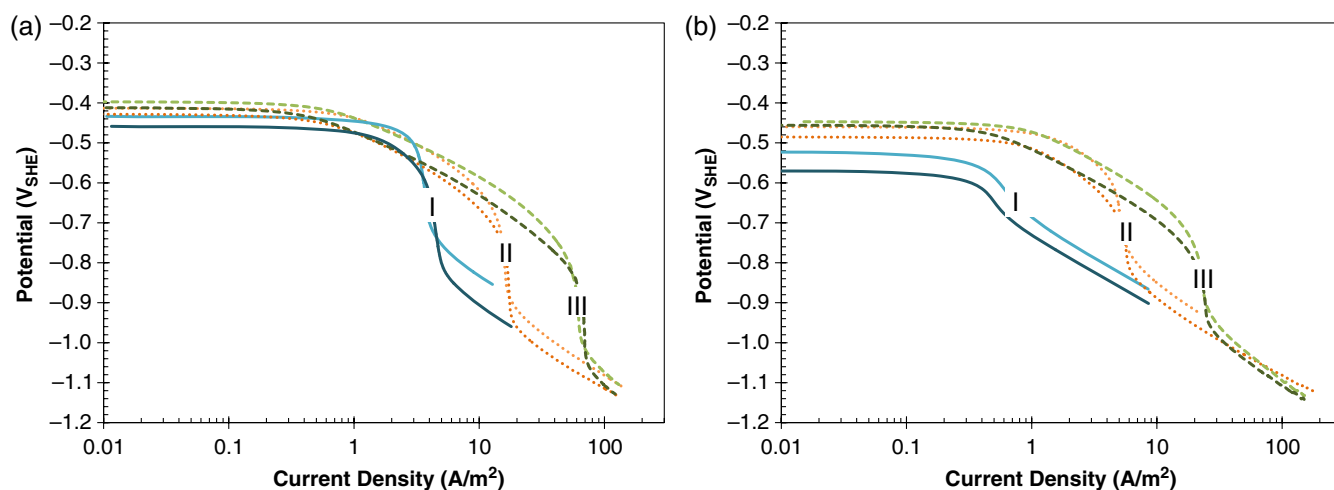


FIGURE 6. Comparison of the polarization curves obtained on iron (dark shades) and X65 steel (light shades) at 25°C, 2,000 rpm RDE, 1 wt% NaCl, and various total acetate concentrations. I: 0 mM, II: 1.66 mM, and III: 8.30 mM. (a) pH 4 and (b) pH 5.

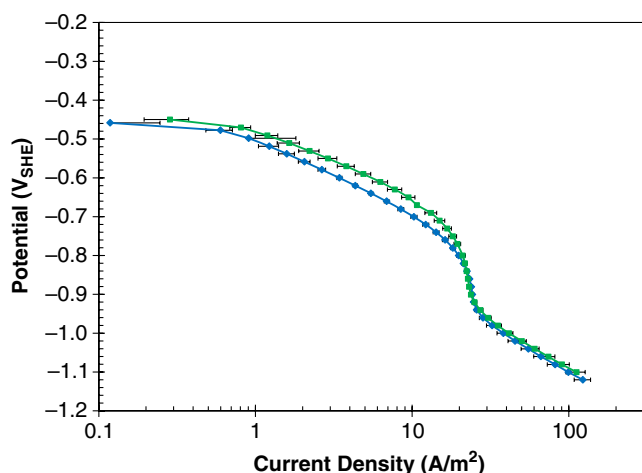


FIGURE 7. Repeatability of the polarization curves at pH 5, 8.30 mM total acetate concentration, 25°C, 2,000 rpm RDE, and 1 wt% NaCl on pure iron (blue diamonds) and X65 mild steel (green squares) at selected potentials. Error bars represent the standard deviation of at least three measurements.

CONCLUSIONS

❖ The behavior of cathodic currents on pure iron and X65 mild steel in mildly acidic sodium chloride solutions containing acetic acid was investigated. The pure charge transfer controlled cathodic currents observed in the experimental data showed no significant response to increasing acetic acid concentration, indicating that direct acetic acid reduction was not significant at the conditions covered in this study. The increase in the limiting current density in the presence of acetic acid was in linear correlation with undissociated acetic acid concentration, as expected from the Levich equation, suggesting that the surface concentration of this species

is negligible at limiting currents. The similar cathodic behavior observed on pure iron and X65 mild steel suggests that the mechanism of the hydrogen evolution reactions was the same on both surfaces.

ACKNOWLEDGMENTS

The authors would like to acknowledge the financial support from Anadarko, Baker Hughes, BP, Chevron, China National Offshore Oil Corporation, CNPC Tubular Goods Research Center, ConocoPhillips, DNV GL, ExxonMobil, M-I SWACO, Occidental Oil Company, Petroleum Institute, PTT, Saudi Aramco, Shell Global Solutions, SINOPEC, TOTAL, TransCanada, and WGK under a joint industrial research project. The authors are also grateful for constructive comments and discussions with Dr. D. Young, Ohio University.

REFERENCES

1. E. Remita, B. Tribollet, E. Sutter, V. Vivier, F. Ropital, J. Kittel, *Corros. Sci.* 50 (2008): p. 1433-1440.
2. T. Tran, B. Brown, S. Nešić, B. Tribollet, *Corrosion* 70 (2014): p. 223-229.
3. Y. Zheng, B. Brown, S. Nešić, *Corrosion* 70 (2014): p. 351-365.
4. L.G.S. Gray, B.G. Anderson, M.J. Danysh, P.R. Tremaine, "Mechanisms of Carbon Steel Corrosion in Brines Containing Dissolved Carbon Dioxide At pH 4," CORROSION 1989, paper no. 464 (Houston, TX: NACE International, 1989).
5. M. Nordsveen, S. Nešić, R. Nyborg, A. Stangeland, *Corrosion* 59 (2003): p. 443-456.
6. B. Tribollet, J. Kittel, A. Meroufel, F. Ropital, F. Grosjean, E.M.M. Sutter, *Electrochim. Acta* 124 (2014): p. 46-51.
7. J. Kittel, F. Ropital, F. Grosjean, E.M.M. Sutter, B. Tribollet, *Corros. Sci.* 66 (2013): p. 324-329.
8. S. Nešić, J. Postlethwaite, S. Olsen, *Corrosion* 52 (1996): p. 280-294.
9. C. de Waard, D.E. Milliams, *Corrosion* 31 (1975): p. 177-181.
10. S. Nešić, "Carbon Dioxide Corrosion of Mild Steel," in *Uhlig's Corrosion Handbook*, ed. R.W. Revie, 3rd ed. (Hoboken, NJ: John Wiley & Sons, 2011), p. 229-245.
11. P. Menaul, *Oil Gas J.* 43 (1944): p. 80-81.
12. T. Barth, *Appl. Geochem.* 6 (1991): p. 1-15.

13. Y.M. Gunaltun, D. Larrey, "Corrolation of Cases of Top of the Line Corrosion with Calculated Water Condensation Rates," CORROSION 2000, paper no. 71 (Houston, TX: NACE, 2000).
14. T.R. Utvik, *Chemosphere* 39 (1999): p. 2593-2606.
15. J.-L. Crolet, N. Thevenot, A. Dugstad, "Role of Free Acetic Acid on the CO₂ Corrosion of Steels," CORROSION 1999, paper no. 24 (Houston, TX: NACE, 1999).
16. J. Amri, E. Gulbrandsen, R.P. Nogueira, *Corrosion* 66 (2010): p. 035001-1 to 035001-7.
17. J.-L. Crolet, M.R. Bonis, "Why so Low Free Acetic Acid Thresholds in Sweet Corrosion at Low pCO₂?" CORROSION 2005, paper no. 272 (Houston, TX: NACE, 2005).
18. S. Nešić, W. Sun, "Corrosion in Acid Gas Solutions," in *Shreir's Corrosion*, ed. T.J.A. Richardson (Amsterdam, The Netherlands: Elsevier, 2010), p. 1270-1298.
19. M. Singer, D. Hinkson, Z. Zhang, H. Wang, S. Nešić, *Corrosion* 69 (2013): p. 719-735.
20. S.D. Zhu, A.Q. Fu, J. Miao, Z.F. Yin, G.S. Zhou, J.F. Wei, *Corros. Sci.* 53 (2011): p. 3156-3165.
21. Y. Garsany, D. Pletcher, B. Hedges, *J. Electroanal. Chem.* 538-539 (2002): p. 285-297.
22. K.S. George, S. Nešić, *Corrosion* 63 (2007): p. 178-186.
23. K. George, S. Nešić, C. de Waard, "Electrochemical Investigation and Modeling of Carbon Dioxide Corrosion of Carbon Steel in the Presence of Acetic Acid," CORROSION 2004, paper no. 379 (Houston, TX: NACE, 2004).
24. E. Gulbrandsen, "Acetic Acid and Carbon Dioxide Corrosion of Carbon Steel Covered with Iron Carbonate," CORROSION 2007, paper no. 322 (Houston, TX: NACE, 2007).
25. E. Gulbrandsen, K. Bilkova, "Solution Chemistry Effects on Corrosion of Carbon Steels in Presence of CO₂ and Acetic Acid," CORROSION 2006, paper no. 364 (Houston, TX: NACE, 2006).
26. J. Amri, E. Gulbrandsen, R.P. Nogueira, "Role of Acetic Acid in CO₂ Top of the Line Corrosion of Carbon Steel," CORROSION 2011, paper no. 329 (Houston, TX: NACE, 2011).
27. Y. Garsany, D. Pletcher, B. Hedges, "The Role of Acetate in CO₂ Corrosion of Carbon Steel: Has the Chemistry Been Forgotten?" CORROSION 2002, paper no. 273 (Houston, TX: NACE, 2002).
28. P.C. Okafor, B. Brown, S. Nešić, *J. Appl. Electrochem.* 39 (2009): p. 873-877.
29. Y. Sun, K. George, S. Nešić, "The Effect of Cl⁻ and Acetic Acid on Localized CO₂ Corrosion in Wet Gas Flow," CORROSION 2003, paper no. 327 (Houston, TX: NACE, 2003).
30. V. Fajardo, C. Canto, B. Brown, S. Nešić, "Effects of Organic Acids in CO₂ Corrosion," CORROSION 2007, paper no. 319 (Houston, TX: NACE, 2007).
31. M. Matos, C. Canhoto, M.F. Bento, M.D. Geraldo, *J. Electroanal. Chem.* 647 (2010): p. 144-149.
32. Z. Jia, X. Li, C. Du, Z. Liu, J. Gao, *Mater. Chem. Phys.* 132 (2012): p. 258-263.
33. A. Kahyarian, M. Singer, S. Nešić, *J. Nat. Gas Sci. Eng.* 29 (2016): p. 530-549.
34. S. Turgoose, R.A. Cottis, K. Lawson, "Modeling of Electrode Processes and Surface Chemistry in Carbon Dioxide Containing Solutions," in *Computer Modeling in Corrosion*, ed. R.S. Munn, ASTM STP 1154 (West Conshohocken, PA: ASTM International, 1992), p. 67-81.
35. B.F.M. Pots, "Mechanistic Models for the Prediction of CO₂ Corrosion Rates Under Multi-Phase Flow Conditions," CORROSION 1995, paper no. 137 (Houston, TX: NACE, 1995).
36. S. Nešić, M. Nordsveen, R. Nyborg, A. Stangeland, "A Mechanistic Model for CO₂ Corrosion with Protective Iron Carbonate Films," CORROSION 2001, paper no. 040 (Houston, TX: NACE, 2001).
37. S. Nešić, *Corros. Sci.* 49 (2007): p. 4308-4338.
38. C. de Waard, U. Lotz, A. Dugstad, "Influence of Liquid Flow Velocity on CO₂ Corrosion: A Semi-Empirical Model," CORROSION 1995, paper no. 128 (Houston, TX: NACE, 1995).
39. S. Nešić, G.T. Solvi, J. Enerhaug, *Corrosion* 51 (1995): p. 773-787.
40. T. Tran, B. Brown, S. Nešić, "Corrosion of Mild Steel in an Aqueous CO₂ Environment—Basic Electrochemical Mechanisms Revisited," CORROSION 2015, paper no. 671 (Houston, TX: NACE, 2015).
41. S. Navabzadeh, B. Brown, S. Nešić, *Corrosion* 72 (2016): p. 1220-1222.
42. B. Beverskog, I. Puigdomenech, *Corros. Sci.* 38 (1996): p. 2121-2135.
43. A.J. Bard, L.R. Faulkner, *Electrochemical Methods: Fundamentals and Applications* (Hoboken, NJ: John Wiley & Sons, Inc., 2001).
44. J.O. Bockris, D. Drazic, *Electrochim. Acta* 7 (1962): p. 293-313.